Transmission of photonic crystal coupled-resonator waveguide (PhCCRW) structure enhanced via mode matching

Chongjun Jin[1], Nigel P Johnson[1], Harold M H Chong[1], Aju S Jugessur[1,2], Stephen Day[3], Dominic Gallagher[3] and Richard M De La Rue[1]

[1] *Optoelectronics Research Group, Department of Electronics and Electrical Engineering, University of Glasgow, Glasgow G12 8QQ, Scotland, UK*
c.jin@elec.gla.ac.uk
[2]*Department of Electrical and Computer Engineering, McGill University, Montreal H3A 2A7,Canada*
[3] *Photon Design, www.photond.com*

Abstract: A method for increasing the coupling efficiency between ridge optical waveguides and PhCCRWs is described. This increase is achieved via W1 channel waveguide sections, formed within a two-dimensional triangular lattice photonic crystal using mode-matching. The mode-matching is achieved by low quality-factor modified cavities added to both the input and output ports of the PhCCRW. A three dimensional finite-difference time-domain method has been used to simulate light propagation through the modified PhCCRW. We have fabricated PhCCRWs working at 1.5μm in silicon-on-insulator material. Measurements and simulations show that the overall transmission is improved by a factor of two.

OCIS codes: (230.4000) Microstructure fabrication, (130.120) integrated optics devices

References and links

1. A. Yariv, Y. Xu, R. K. Lee, and A. Scherer, "Coupled-resonator optical waveguide: a proposal and analysis," Opt. Lett. **24**, 711-713 (1999).
2. N. Stefanou and A. Modinos, "Impurity bands in photonic insulators," Phys. Rev. B **57**, 12127-12133 (1998).
3. S. Olivier, C. Smith, M. Rattier, H. Benisty, C. Weisbuch, T. Krauss, R. Houdre, and U. Oesterle, "Miniband transmission in a photonic crystal coupled-resonator optical waveguide," Opt. Lett. **26**, 1019-1021 (2001).
4. T. J. Karle, D. H. Brown, R. Wilson, M. Steer, and T. F. Krauss, "Planar photonic crystal coupled cavity waveguides**,"** IEEE J. Sel. Top. Quantum Electron. **8**, 909-918 (2002).
5. A. Martínez, A. García, P. Sanchis, J. Martí, "Group velocity and dispersion model of coupled-cavity waveguides in photonic crystals," J. Opt. Soc. Am. A **20**, 147-150 (2003).
6. T. J. Karle, Y. J. Chai, C. N. Morgan, I. H. White, and T. F. Krauss, "Observation of Pulse Compression in Photonic Crystal Coupled Cavity Waveguides," J. Lightwave Technol. **22**, 514-519 (2004).
7. S. Mookherjea, A. Yariv, "Kerr-stabilized super-resonant modes in coupled-resonator optical waveguides," Phys. Rev. E **66**, 046610-046616 (2002).
8. S. Mookherjea, A. Yariv, "Coupled Resonator Optical Waveguides," IEEE J. Sel. Top. Quantum Electron. **8**, 448-456 (2002).
9. S. Mookherjea, D. S. Cohen, and A. Yariv, "Nonlinear dispersion in a coupled-resonator optical waveguide," Opt. Lett. **27**, 933-935 (2002).
10. S. Mookherjea, A. Yariv, "Second-harmonic generation with pulses in a coupled-resonator optical waveguide," Phys. Rev. E **65**, 026607-026615 (2002).
11. M. Bayindir and E. Ozbay, "Band-dropping via coupled photonic crystal waveguides," Opt. Express **10**, 1279-1284 (2002). http://www.opticsexpress.org/abstract.cfm?URI=OPEX-10-22-1279
12. M. Bayindir, B. Temelkuran, and E. Ozbay, "Photonic crystal based beam splitters," Appl. Phys. Lett. **77**, 3902-3904 (2000).
13. H. M. H. Chong and R. M. De La Rue, **"**Tuning of photonic crystal waveguide microcavity by thermooptic effect," IEEE Photon. Technol. Lett. **16**, 1528-1530 (2004).
14. A. S. Jugessur, P. Pottier and R. M. De La Rue, "One-dimensional photonic crystal microcavity filters with transition mode-matching features, embedded in ridge waveguide," Electron. Lett. **39**, 367-369 (2003).
15. A. S. Jugessur, P. Pottier and R. M. De La Rue, "Engineering the filter response of photonic crystal microcavity filters," Opt. Express **12**, 1304-1312 (2004). http://www.opticsexpress.org/abstract.cfm?URI=OPEX-12-7-1304

#6144 - $15.00 US Received 23 December 2004; revised 14 March 2005; accepted 15 March 2005

16. J. P. Berenger, "Three-dimensional perfectly matched layer for the absorption of electromagnetic waves," J. Comput. Phys. **127,** 363-379 (1996).
17. A. Lavrinenko and D. Gallagher, "CrystalWave", Photon Design, www.photond.com, developed under European Framework 5 Project "PICCO", (2003).
18. K. Srinivasan and O. Painter, "Momentum space design of high-Q photonic crystal optical cavities," Opt. Express **10**, 670-684 (2002). http://www.opticsexpress.org/abstract.cfm?URI=OPEX-10-15-670
19. H. Ryu, M. Notomi, G. Kim and Y. Lee, "High quality-factor whispering-gallery mode in the photonic crystal hexagonal disk cavity," Opt. Express **12**, 1708-1719 (2004). http://www.opticsexpress.org/abstract.cfm?URI=OPEX-12-8-1708
20. A.J. Ward and J.B. Pendry, "A program for calculating photonic band structures, Green's functions and transmission/reflection coefficients using a non-orthogonal FDTD method," Computer Physics Communications **128** 590-621 (2000).
21. A. Lavrinenko, P. I. Borel, L. H. Frandsen, M. Thorhauge, A. Harpth, M. Kristensen, T. Niemi, H. M. H. Chong, "Comprehensive FDTD modelling of photonic crystal waveguide components," Opt Express **12**, 234-248 (2004). http://www.opticsexpress.org/abstract.cfm?URI=OPEX-12-2-234

1. Introduction

A Photonic Crystal (PhC) Coupled-Resonator Waveguide (CRW) is a waveguide composed of a sequence of linked photonic crystal cavities [1-4]. Such a waveguide can serve as a strongly wavelength dependent delay-line [5], can be used for pulse compression [5,6] - and can also be used to enhance nonlinear effects such as second-harmonic generation [5,7-10]. Due to its modal symmetry, the hexagonal photonic crystal CRW can be bent through 60^{o} without, in principle, any reflection [1]. It can also be useful as a form of wavelength-demultiplexer [11-12]. The CRW is attractive because of its potential applications in integrated optoelectronic circuits. However, as the name implies, because this waveguide structure has strongly resonant behaviour, coupling light efficiently into and out of the CRW remains a challenge. To the best of our knowledge, there are no reports of techniques specifically designed to increase the coupling efficiency between CRWs and ridge or PhC channel optical waveguides, except for the case of coupling to a single cavity [13]. We report here on structural modifications that increase the coupling efficiency between CRWs, embedded in W1 PhC channel guides, and ridge waveguides using mode-matching[14,15]. The finite-difference time domain (FDTD) method was used to simulate the optical propagation in the modified CRWs. It has been found that, by the addition of matching, low quality-factor ('low–Q'), cavities, the coupling efficiency can be doubled and consequently the transmission can be substantially improved. The modified cavities are formed firstly from a reduction of the size of the outer holes - and secondly by the insertion of a small additional hole into the outer cavities at the input and output ports of a CRW structure (see Fig. 1). To confirm the influence of using mode-matching cavities, CRWs were fabricated in silicon-on-insulator wafers both with and without the cavity modifications. Measurements show that, when the matching cavities are added to both ports of the CRW, the transmission can be increased substantially over the wavelength region of interest.

In a photonic crystal coupled-resonator waveguide, light typically propagates into a highly resonant waveguide from a ridge waveguide. Usually this is accompanied by a very strong reflection, because of the large mismatch, both in modal distribution and wave impedance. Here we propose that light should firstly enter and leave the CRW via W1 (one missing line-of-holes) PhC channel waveguides. In general, a W1 channel waveguide that is 7 lattice constants in length is sufficient to ensure that light will be fully coupled into the W1 channel waveguide and propagate as the dominant, even-symmetry, W1 channel waveguide mode. Subsequently the propagating mode will be changed to the propagation mode of the CRW. To facilitate this change of propagation mode, a low-Q, resonance frequency-shifted, asymmetric cavity is added to each interface between the W1 channel waveguide and the CRW as shown in Fig. 1. At each end of the device the cavity is formed by two smaller holes and one normal hole (shared with the CRW). The first smaller hole (labelled A in the figure), as encountered by the W1 channel guided input wave, is larger than the second (labelled B in the figure). This

#6144 - $15.00 US Received 23 December 2004; revised 14 March 2005; accepted 15 March 2005

two-step approach reduces the modal mismatch in the system, with the B-type hole perturbing substantially the resonant mode through its location in the middle of the matching cavity. Because the CRW is a strongly resonant waveguide, there will be significant vertical leakage that will lead to increased loss as the number of cavities forming the CRW increases.

The structure is based upon a triangular (hexagonally symmetric) planar photonic crystal formed by air holes in a silicon-on-insulator wafer. Because it is relatively easy to open a large band-gap for TE polarized light (for which the electrical field is predominantly perpendicular to the axes of the holes) in such a system, only the TE modal behaviour has been considered in this paper.

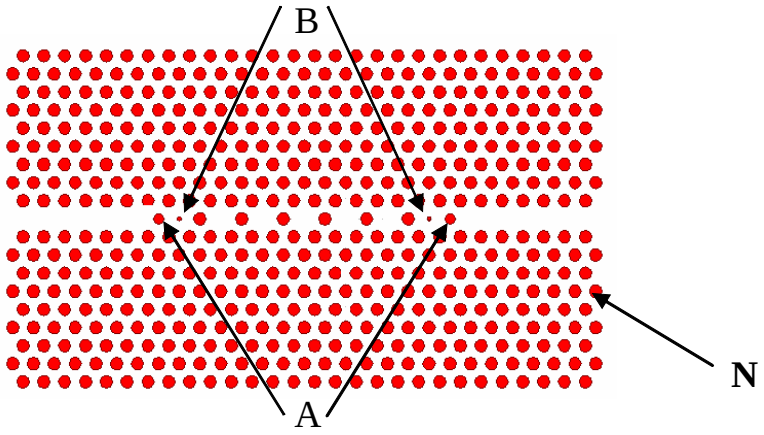

Fig. 1. A photonic crystal CRW with modified end cavities. The diameter of the outer holes (A) is 79 % of the diameter of holes that form the majority of the crystal (N). The diameter of the holes modifying the end cavities (B) is 42 % of the diameter of N.

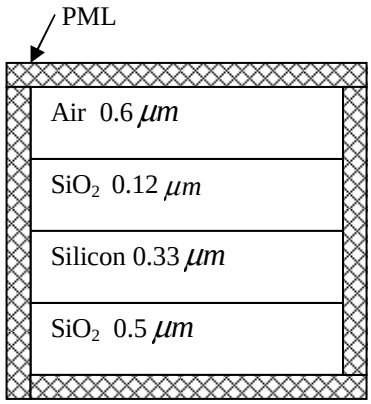

Fig. 2. The transverse cross-section of the basic vertical confinement structure, with propagation normal to the plane of the diagram.

The planar triangular photonic crystal used in our simulation was fabricated in an asymmetrical planar waveguide structure. The cross-section used in the modelling of the planar (vertical confinement) waveguide is shown in Fig. 2, which is only used for modelling work and incorporates a perfectly matched layer (PML) at all boundaries of the device structure [16,17]. To reduce the computation time, the actual interface between the lower silica cladding layer and the silicon substrate is neglected. There are four layers. The first layer is air simulated with a thickness of 0.6μm. The second layer is the top cladding, composed of a thickness of 0.12μm of silica with a refractive index of 1.45. The third layer is

#6144 - $15.00 US Received 23 December 2004; revised 14 March 2005; accepted 15 March 2005

the silicon core layer, with thickness and refractive index of 0.33μm and 3.45 respectively. The final layer is the bottom cladding of silica, with a thickness of 0.5μm. The depth of the holes was around 0.5μm, penetrating through the core layer and entering into the bottom cladding to a depth of approximately 50nm.

2. Simulations

Two-dimensional (2D) FDTD simulations cannot take account of vertical leakage, as was confirmed by initial 2D simulation studies that showed a broad flat response unlike that of measured devices. Three-dimensional (3D) FDTD simulations are now routinely employed in simulations of cavity structures [18,19]. In this paper, 3D-FDTD simulations have been performed using an implementation of the finite-difference time-domain algorithm [17]. An alternating forward-difference/backward-difference discretisation of Maxwell's Equations was employed, as developed by Ward and Pendry [20]. In fact our recent analysis [21] of the Ward/Pendry algorithm suggests that it becomes equivalent to the more widely known Yee algorithm [22], if one shifts certain fields of the Ward/Pendry algorithm by a half-space step, as shown in Fig. 3.

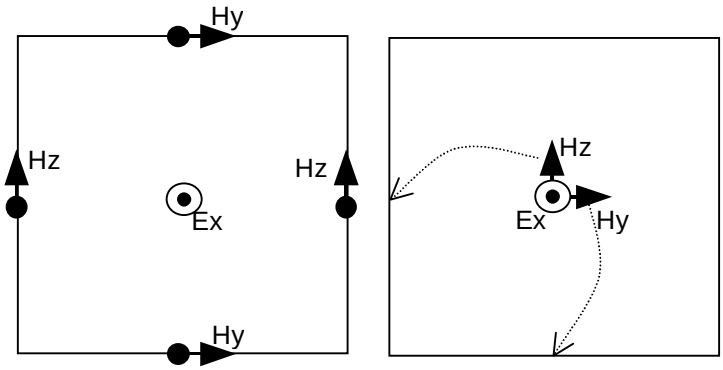

Fig. 3. The Yee scheme (on the left), showing staggering of the E_x, H_y and H_z fields. (In 2D only{E_x, H_y, H_z} or {H_x, E_y, E_z} need to be considered, depending on the polarisation of the launched light). On the right is the Ward/Pendry scheme, where fields are unstaggered but a forward-difference/backward-difference step in the evolution algorithm is applied in alternation. The dotted arrows show how the Ward/Pendry fields can be displaced to arrive at an equivalent of the Yee scheme. Though more complex, an equivalent displacement process can be applied to the 3D algorithm.

Figure 4 shows the simulated spectra for the CRW composed of 9 cavities. The solid and dashed lines represent the spectra of CRW1 and CRW2, with and without matching cavities respectively. The radius R for the holes comprising the photonic crystal is $0.310\,a$, where a is the lattice constant and has been chosen as $0.42\,\mu m$ in our experiments. The radii of the first and second matching holes are $0.245\,a$ and $0.129\,a$ respectively. In the simulation, we also incorporated a very thin silica wall into the hole to represent possible oxidation and etch-damage effects on the silicon. The chosen thickness of the silica wall is $0.052\,a$. Fig. 4 shows that the pass band is quite large, stretching from $3.5\,a$ to $3.71\,a$. It is clear that the transmitted power of the CRW with matching holes is nearly twice as large, at the centre of the pass band. This behaviour implies that low Q-factor asymmetric and frequency-shifted cavities, placed at both input and output, can help the light enter into and leave the CRW with reduced reflection and leakage. From the shape of the transmission curves, it can be seen that, for the CRW with matching cavities, the band width is reduced compared with the CRW without matching cavities.

#6144 - $15.00 US Received 23 December 2004; revised 14 March 2005; accepted 15 March 2005

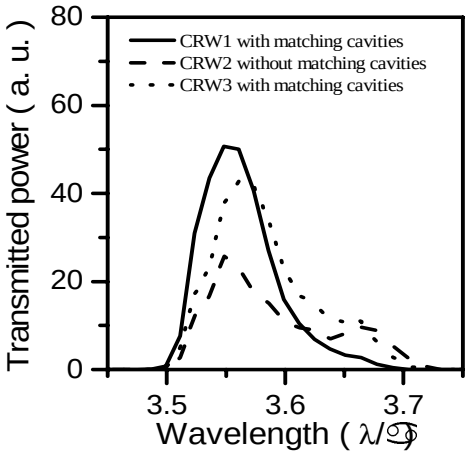

Fig. 4. Spectra of transmitted power of the PhCCRW structures with and without matching cavities, where CRW2 is the coupled-resonator waveguide without matching cavities; CRW1 and CRW3 are coupled-resonator waveguides with matching cavities. The resonance can also be tuned: as the smaller hole is reduced in size the peak moves from shorter (solid line CRW1) to longer wavelength (dotted line CRW3).

The properties of the coupling technique just described also make it easy to tune the maximum in the spectrum by adjusting the resonant peaks of the matching cavities. The dotted line represents the spectrum of a CRW3 with matching cavities, in which the radii of the two matching holes are 0.245 a and 0.107 a respectively. Compared with the structure corresponding to the solid line spectrum (CRW1), the only change is that the radius of the small matching hole decreases, from 0.129 a to 0.107 a. The normalised centre wavelength (λ/a) now moves from 3.555 to 3.565 - and has therefore moved to longer wavelengths as the size of the second matching hole (holes of type B) is reduced. This result arises because, as the modal volume of the cavity becomes larger, the resonant peak wavelength of the matching cavity moves to longer wavelengths. The results of Fig. 4 imply that the central resonance can be tuned by changing the size of the matching holes. However, when the matching holes change in size by more than 20%, the central peak changes its spectral position by only 0.28%, which is useful in the design and fabrication of the CRW because it places less demand on the fabrication tolerances for tuning of the device.

3. Fabrication and measurement

To test the validity of the above design methods, photonic crystal CRWs were fabricated in silicon-on-insulator (SOI) material. The SOI wafer consists of a 340 nm layer of single-crystal silicon forming the waveguide core, on top of a 3 μm thick silica buffer layer on the top of the silicon substrate. A further 200 nm layer of silica was deposited on top of the silicon and served as a dry-etch mask for transfer of the PhCCRW structure into the silicon waveguide core. The pattern was written in a layer of ZEP 520A resist by electron-beam lithography and developed using Oxylene. The resist pattern was transferred into the deposited silica layer using reactive ion etching (RIE) with CHF_3. Finally the pattern was transferred into the silicon layer by RIE using $SiCl_4$. As the holes are not perfectly circular, a thermal oxidation process was employed to oxidize the silicon by a small amount (15nm). This additional process produces a more uniformly shaped hole [13].

Figure 5 is a scanning electron micrograph of the photonic crystal CRW with 9 cavities (after removing SiO_2 mask), the inset shows the CRW matching holes. The diameter of the normal (N) holes is 260 nm, the diameter of the two matching holes are (A) 208 nm and (B)

#6144 - $15.00 US Received 23 December 2004; revised 14 March 2005; accepted 15 March 2005

108 nm, respectively. The profile of the etched holes was also observed. It was found that all but the smallest holes were etched through the whole silicon layer. The normal holes were in fact fully etched through the silicon layer and slightly into the silica layer below. Because of the oxidation process, there was a wall of silica around the holes. The thickness of the wall is about 22 nm, and the thickness of the core (silicon layer) was reduced to 330 nm.

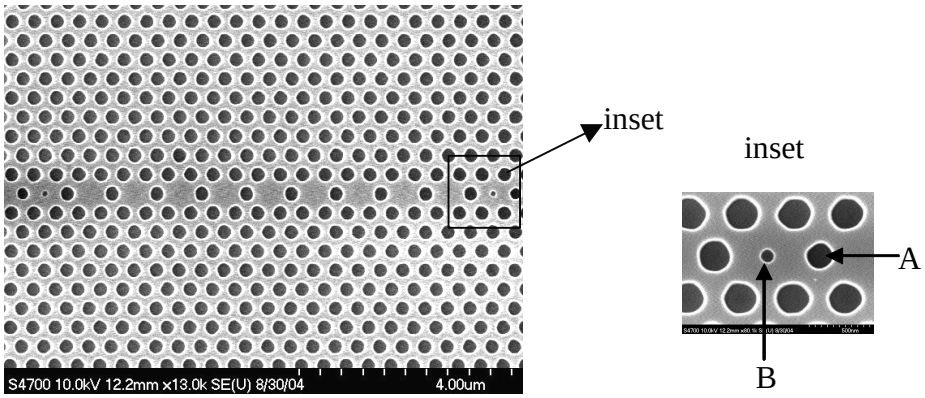

Fig. 5. Scanning electron micrographs of the photonic crystal CRW composed of 9 cavities, with additional input and output matching cavities. The inset shows one of the matching cavity regions, where A and B are the matching holes.

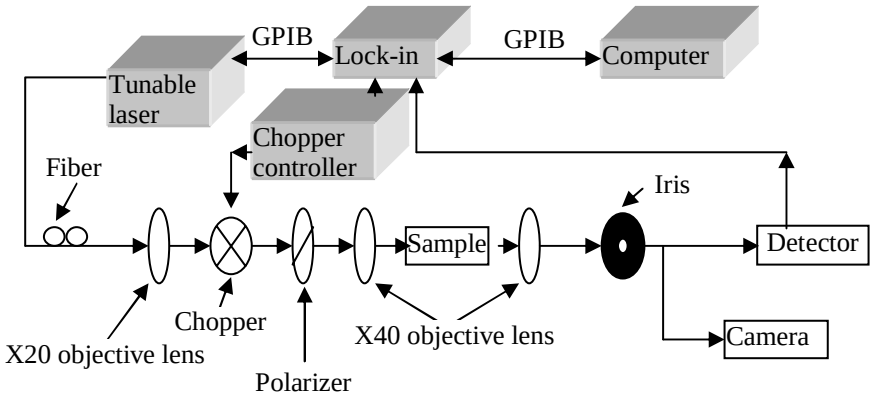

Fig. 6. Schematic measurement set-up. Light from a tunable laser is guided by a fiber and collimated by a $\times 20$ objective lens, chopped, (TE)-polarized and focused onto the input port of the waveguide in the sample by a $\times 40$ objective lens. The light from the output port of the waveguide of the sample was imaged by another $\times 40$ objective lens - and viewed initially by a camera. Subsequently, the output light was detected by a germanium detector. The signal was amplified by a lock-in amplifier, collected at the corresponding wavelength – and recorded on a computer.

#6144 - $15.00 US Received 23 December 2004; revised 14 March 2005; accepted 15 March 2005

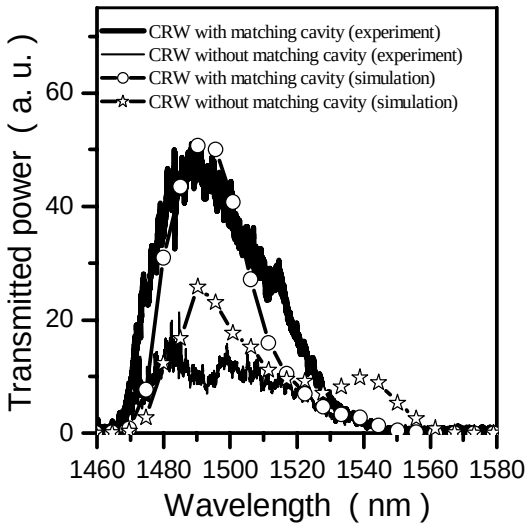

Fig. 7. The transmitted power spectra for the CRW composed of 9 cavities plus two matching cavities shown in Fig. 5, where thick solid and open-circle lines represent the experimental and simulation spectra. The thin solid and starred lines represent the experimental and simulation spectra for the CRW without matching cavities. The simulation results have already been shown in Fig. 4 (CRW1 and CRW2).

The devices were measured by the end-fire coupling method. A schematic setup is shown in Fig. 6. Light from a tunable semiconductor laser was coupled into the input port of a cleaved facet of the sample by an x40 microscope objective - and similarly collected from the output ports of the cleaved facet through another x40 microscope objective. The light was detected by a large area germanium photodiode and the signal was amplified by a lock-in amplifier. The signal and corresponding wavelength were collected by a computer from lock-in amplifier and tunable laser. Fabry-Perot (F-P) resonant phenomena caused by partial reflection between the cleaved facet and the junction of the photonic crystal W1 channel waveguide were present in the measurements. The period of the F-P oscillations was less than 0.2 nm – and, moreover, this phenomenon is not an intrinsic property of the CRW. A Fast-Fourier-Transformation (FFT) filter was used to suppress the effect of the F-P resonance in the measurements. The transmitted power spectra of the CRWs are shown in Fig. 7. The thick and thin solid lines are for the CRWs with and without matching cavities. It is clear that, over almost the whole pass-band, the CRW with matching cavities has a substantially higher transmitted power, even though a longer device could be expected to give less transmission. In particular, the transmitted power of the CRW with matching cavities is nearly three times larger than the one without matching cavities, in the range from 1473 to 1524 nm, and this width is nearly 64% of the whole pass-band. To compare with the simulation results, the simulated transmission spectra are also plotted in Fig. 7. The dotted and starred lines represent the simulated spectra for the transmitted power of the CRWs, with and without matching cavities respectively which has been show in Fig. 4 by CRW1 and CRW2. It is clear that the shape of the spectra of the CRWs is very similar between the simulations and measurements. However, there are several differences. For the CRW without matching cavities, the first peak in the measurement is slightly split, while the second one disappears. For the CRW with matching holes, the experimental bandwidth is wider than the simulated one. These differences between simulation and experiment may be caused by small deviations in the size of the holes from specification and from each other.

The transmission spectra of the CRWs can also be normalized with respect to a ridge waveguide. It was observed that, for the above case, the highest transmission can be over 13%

#6144 - $15.00 US Received 23 December 2004; revised 14 March 2005; accepted 15 March 2005

for the CRW with matching cavities. It was found that the transmission is strongly related to the number of cavities composing the CRW. Characteristically the more cavities that are used, the lower the transmission obtained. This is probably because the total level of diffuse scattering and leakage from the imperfect structure increases with the device length.

4. Conclusions

A method for enhancing the coupling efficiency between ridge and photonic-crystal coupled-resonator waveguides has been demonstrated by adding an extension W1 channel waveguide and matching low-Q cavities at both the input and the output ports of the CRW. The simulation and experiment results show that the transmission can be increased by a factor of two through this addition to the structure. The results are also robust with respect to small changes in the size of matching holes. The experimental and simulated results show generally good agreement. The use of matching cavities will be a valuable tool in the design of CRW waveguides to be used in integrated-optical circuits.

Acknowledgments

We acknowledge the support of the EPSRC grant GR/R35681/01

#6144 - $15.00 US Received 23 December 2004; revised 14 March 2005; accepted 15 March 2005